November 2016

The Role of MicroRNAs in Regulating the Translatability and Stability of Target Messenger RNAs During the Atrophy and Programmed Cell Death of the Intersegmental Muscles of the Tobacco Hawkmoth Manduca sexta.

Elizabeth Chan
University of Massachusetts Amherst

THE ROLE OF MICRORNAS IN REGULATING THE TRANSLATABILITY AND STABILITY OF TARGET MESSENGER RNAS DURING THE ATROPHY AND PROGRAMMED CELL DEATH OF THE INTERSEGMENTAL MUSCLES OF THE TOBACCO HAWKMOTH *MANDUCA SEXTA*

A Thesis Presented

by

ELIZABETH CHAN

Submitted to the Graduate School of the University of Massachusetts Amherst in partial fulfillment of the requirements for the degree of

MASTER OF SCIENCE

September 2016

Molecular and Cellular Biology

THE ROLE OF MICRORNAS IN REGULATING THE TRANSLATABILITY AND STABILITY OF TARGET MESSENGER RNAS DURING THE ATROPHY AND PROGRAMMED CELL DEATH OF THE INTERSEGMENTAL MUSCLES OF THE TOBACCO HAWKMOTH *MANDUCA SEXTA*

A Thesis Presented

By

ELIZABETH CHAN

Approved as to style and content by:

_____
Lawrence M. Schwartz, Chair

_____
Li-Jun Ma, Member

_____
Leonid Pobezinsky, Member

_____
Elizabeth R. Dumont, Director,
Interdepartmental Graduate Programs, CNS

ACKNOWLEDGEMENTS

First and foremost, I would like to acknowledge Professor Lawrence Schwartz for accepting me into the Schwartz lab as an undergraduate student at UMass Amherst and entrusting me with my own research project. Professor Schwartz has been and continues to be a great mentor and teacher in all aspects of my life. I would also like to acknowledge Christine Brown for taking time to train me as an undergraduate and equipping me with many of the lab skills I have today. Also, I would like to thank her for taking time to guide me through difficult protocols. I would also like to thank all the members of the Schwartz lab for providing feedback during lab meetings and helping with my project in the past 3 years, especially Joanne Johnson, Varun Sheel, Khaled Said, Justyne Ogdahl, Alice Richardson and Ankur Sheel. I would also like to acknowledge Junko Tsuji for her help with the bioinformatics data.

This project would also not have been possible without my committee members: Professor Ma and Professor Pobezinsky. I would like to acknowledge Professor Ma for accepting to be on my committee twice as well as her guidance in data presentation and analysis. I would also like to acknowledge Professor Pobezinsky for all his guidance in navigating the complexity of microRNAs as well as helping me troubleshoot my experiments.

Finally, I would like to thank my parents, friends and family for encouraging me to reach my highest potential.

ABSTRACT

THE ROLE OF MICRORNAS IN REGULATING THE TRANSLATABILITY AND STABILITY OF TARGET MESSENGER RNAS DURING THE ATROPHY AND PROGRAMMED CELL DEATH OF THE INTERSEGMENTAL MUSCLES OF THE TOBACCO HAWKMOTH *MANDUCA SEXTA*

SEPTEMBER 2016

ELIZABETH CHAN, B.S., UNIVERSITY OF MASSACHUSETTS AMHERST

M.S., UNIVERSITY OF MASSACHUSETTS AMHERST

Directed by: Professor Lawrence Schwartz

A variety of diseases lead to the atrophy and/or death of skeletal muscle. To better understand the molecular mechanisms that mediate these processes, I have taken advantage of the intersegmental muscles (ISMs) of the tobacco hawkmoth *Manduca sexta*, which undergo sequential programs of atrophy and programmed cell death at the end of metamorphosis. ISM death is mediated by changes in gene expression and numerous cell-death associated transcripts have been identified. MicroRNAs (miRs) are small (~22 nucleotide) non-coding RNAs that bind to sequences in messenger RNAs (mRNAs) and either cause translational arrest or mRNA degradation. To test the hypothesis that developmentally regulated miRs may control the stability and/or translatability of target mRNAs in the ISMs, putative mRNA targets for the test miRs have been identified and their 3' untranslated region (UTR) have been cloned into a dual luciferase reporter plasmid. The microRNA mir-92b binds to the 3' UTR of the Small Cytoplasmic Leucine Rich repeat Protein (SCLP) mRNA. Expression of miR-92b declines during development and SCLP expression increases with the commitment to die. I found that the miR-92b inhibits luciferase mRNA translation (spectrophotometric plate assays), but does not lead to transcript degradation (quantitative polymerase chain

reaction; qPCR). miR-92 plays a survival role in several mammalian tissues and is repressed in two types of cardiomyopathy. Consequently, understanding how miRs regulate mRNA translation and stability may provide a better understanding of the regulation of muscle atrophy and death as well as provide novel tools for diagnostics or therapeutics.

TABLE OF CONTENTS

Page

LIST OF FIGURES

CHAPTER I

THE ROLE OF MICRORNAS IN REGULATING THE TRANSLATABILITY AND STABILITY OF TARGET MESSENGER RNAS DURING THE ATROPHY AND PROGRAMMED CELL DEATH OF THE INTERSEGMENTAL MUSCLES OF THE TOBACCO HAWKMOTH *MANDUCA SEXTA*

Introduction

Skeletal muscle is the largest tissue in the body and serves as its primary reservoir of amino acids. During development or following exercise, muscles can undergo hypertrophy resulting in increased mass, while starvation and certain disorders can result in a net loss of muscle protein, a condition known as atrophy. Some of the factors that can induce atrophy include: diabetes, cancer cachexia, motor neuron diseases, spinal cord injury, immobility, and aging (Schiaffino et al., 2013). Age-associated atrophy, known as sarcopenia, is a condition that causes protracted atrophy and a decrease in strength in the elderly (Leeuwenburgh and Marzetti, 2006). Sarcopenia affects 13-24% of 50 year olds and up to 50% of people over age 80 (Baumgartner et. al., 1999). These individuals lose muscle mass at a rate of 1-2% per year, which means that they may lose up to 40% of their muscle mass by age 80, resulting in physical disabilities, decrease in independence, and increased risk of falls (Hughes et al., 2002; Roubenoff, 2000). Sarcopenia takes a major toll on both the quality of life and the national economy (Janssen et al, 2004). Despite the prevalence of sarcopenia, there is still much to be learned about the regulatory processes that lead to the dramatic decrease of muscle mass. Physical inactivity and declines in certain hormones may play roles, although the underlying molecular mechanisms are poorly understood (Dirks and Leeuwenburgh, 2002; Szulc et al., 2004).

Given the slow progression of sarcopenia and many other muscle disorders, it is challenging to study skeletal muscle atrophy and muscle fiber cell death in humans. An alternative strategy is to utilize a model system where it is easier to identify the underlying molecular mechanisms that can inform subsequent clinical studies. One such model is the intersegmental muscle (ISM) of the tobacco hawkmoth *Manduca sexta* (Schwartz, 2008).

Late in metamorphosis the ISMs initiate a program of atrophy that results in a 40% loss of muscle mass over a three-day period (Schwartz and Truman, 1983). The muscles are then used to eclose (emerge) from the overlying pupal cuticle at the end of metamorphosis allowing the moth to escape. Concurrent with eclosion, the ISMs initiate programmed cell death (PCD) and die during the subsequent 30 hours (Lockshin and Williams, 1965; Schwartz, 2008). The ISMs have a number of additional properties that make them attractive models for the study of atrophy and cell death. Unlike mammalian muscles, the ISMs are composed of a single fiber type and lack regenerative muscle stem cells (satellite cells), all of which help overcome some of the technical limitations that are associated with studying heterogeneous tissues (Schwartz, 2008).

There are four stages associated with the changes in ISMs physiology and development observed at the end of metamorphosis: homeostasis (prior to the onset of atrophy), atrophy, committed to die, and actively dying (Schwartz and Ruff, 2002). During homeostasis, which lasts until day 15 of the normal 18 days of pupal-adult development, the ISMs are intact, fully functional and display a constant mass (Schwartz and Truman, 1983). Between days 15 and 18 the ISMs undergo atrophy and lose 40% of their mass, which results from decreased expression of the genes that encode contractile

proteins as well as enhanced ubiquitin-dependent proteolysis (Schwartz et. al., 1993; Schwartz and Ruff, 2002). Following eclosion, the muscles activate a different program that results in the complete derangement of the contractile apparatus and the destruction of the fibers. These changes in muscle mass and structure can be readily seen in images of the isolated ISMs at different stages of development (Figure 1).

The ability of the ISMs to die is dependent on *de novo* gene expression (Schwartz et al., 1990a). Between days 17 and 18 there are dramatic changes in the patterns of gene expression within the ISMs that coincide with the commitment of the cells to die (Schwartz et al., 1990). Some of the primary patterns of differential gene expression can be seen via Northern blot analyses for polyubiquitin, the myosin heavy chain and small cytoplasmic leucine rich repeat (SCLP) (Figure 2) (Schwartz, 2008). While some transcripts are seen to increase, including polyubiquitin, proteasome subunits, and Acheron, others are repressed, for example actin and myosin heavy chain (Schwartz et al., 1993).

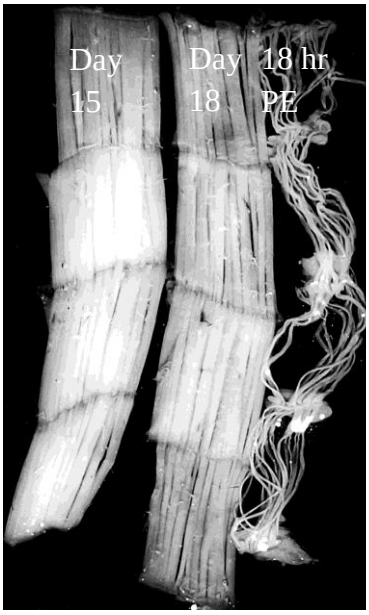

Figure 1. Isolated ISMs during different stages of development. Prior to day 15, the ISMs are intact and have initiated atrophy. Between days 15 and 18 of pupal-adult development, the ISMs have undergone atrophy and lost ~40% of their mass. On day 18, the ISMs are committed to die and are used for adult eclosion. 18 hours post eclosion (PE) there is a dramatic loss of muscle mass as the ISMs die.

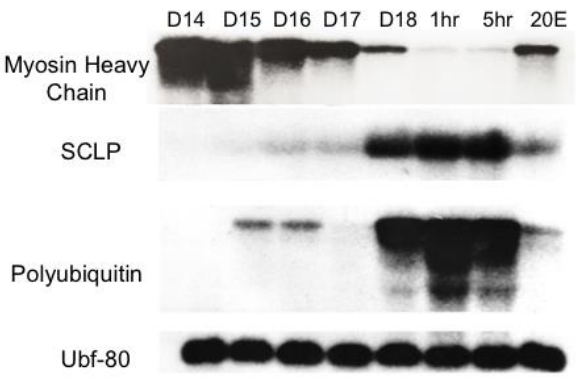

Figure 2. Northern blot of developmentally regulated genes during ISM development. The myosin heavy chain is one of the major contractile proteins. Its expression declines during atrophy. During ISM atrophy and death, there is a dramatic induction of SCLP and polyubiquitin on day 18 when the muscle is committed to die. However, the majority of genes are not differentially expressed, including the Ubf-80 (ubiquitin fusion 80 gene), which is constitutively expressed. A decline in the serum levels of 20 hydroxyecdysone hormone (20E) triggers the changes in gene expression, therefore when we treat the *Manduca* with 20E, muscle death is delayed.

These changes in transcript abundance predominantly reflect changes in transcription. However, there are some intriguing data that suggest that RNA stability may also decrease on day 17 (Cascone and Schwartz, 2001). The instability of the RNAs may serve to help allow the cell to shift from one developmental program to another by removing "housekeeping" transcripts at a time when cell death-associated RNAs are being induced. The mechanisms that mediate changes in transcript abundance and stability when the ISM transition from atrophy to death programs are poorly understood. We have also made the intriguing observation that the abundance of proteasome subunits mRNA increases about two-fold from day 16-18, but that the abundance of the corresponding protein increases by a couple orders of magnitude. These data suggest that there are regulatory controls that impact not only transcript abundance but also mRNA translatability. To examine the control of these changes in expression, Cascone and Schwartz demonstrated that there were sequences contained within the 3'UTR of differentially expressed transcripts that control both transcript abundance and stability (Cascone and Schwartz, 2001). While they did not suggest how these sequences are controlled, one likely class of regulators are the microRNAs.

MicroRNAs (miRNAs) are small (~22 nucleotide) non-coding RNAs that bind to specific sequences within mRNAs and regulate their stability and translatability (Bartel, 2009). MicroRNAs can act to cause translational arrest through blocking translational initiation, deadenylation of the poly(A^+) tail, or recruitment of translational blockers (Ameres and Zamore, 2013). They also bind to mRNAs in unique ways. There does not need to be complete complementarity between miRNAs and their mRNA targets to mediate regulation. Instead, there are seed regions that are located at nucleotides 2-8 from the miRNA 5' region, where miRNAs and mRNAs are complementary (Zhang et al., 2013). Partial complementarity results in translational arrest, while extensive complementarity results in mRNA degradation (Hutvagner and Zamore, 2002). Even if the mRNA is not completely complementary to the seed regions, binding at the centered site regions located at nucleotides 4-15 and 5-15 from the 5' region, can also cause translational repression (Zhang et al., 2013). The 3' supplementary sites of miRNA nucleotides 12-16 can also enhance mRNA repression via miRNA binding to the mRNA target (Ameres and Zamore, 2013). Because multiple miRNA binding sites can be found within the same transcript, it is possible for one or a few miRNAs to regulate major developmental pathways in cells, such as mitosis (Bartel, 2009). Consequently, miRNAs may also provide tools for both diagnostics and therapeutics for many diseases (Van Rooij and Olson, 2007).

To test the hypothesis that miRNAs regulate cell death associated transcripts in the ISMs, I have selected four of the conserved genes that are induced when the ISMs become committed to die on day 18: Ubiquitin Carboxyl-Terminal Hydrolase 7 (UCH-

7), Acheron, Trip-1/SUG1, and small cytoplasmic leucine rich repeat protein (SCLP). UCH-7 cleaves polyubiquitin chains and serves to increase the pool of free ubiquitin monomer within cells, which in turn helps facilitate protein degradation (He et al., 2014). Acheron is a survival protein that helps coordinate the timing of ISM death (Valavanis et al., 2007). The Trip-1/SUG1 protein is an ATPase located in the 19S cap of the 26S proteasome, and it helps unwind proteins for ubiquitin-dependent degradation (McKenna et al., 2013). SCLP contains leucine rich repeats and is a death-associated protein although its function in atrophy and death have yet to be defined (Keulzer et al., 1999).

By studying miRNA regulation of mRNA function we will not only generate new insights into the molecular mechanisms controlling skeletal muscle atrophy and death, but also possible targets for therapeutic interventions or diagnostics. For example, by determining the miRNA levels during the four developmental stages in which the ISMs undergo (homeostasis, atrophy, committed to die, and actively dying) as explained above, the miRNA levels might be useful for classifying which developmental stage the ISMs, and possibly diseased muscles are in.

Results

Genes of interest

To gain a better understanding of the control of transcript stability and translatability of genes that are induced when the ISMs of *Manduca* become committed to die on day 18 of development, we chose to analyze UCH-7, Acheron, Trip-1/SUG1, and SCLP (Figure 3). The developmentally regulated miR-2765 has seed regions that are partially complementary to the target regions in the 3'UTRs of UCH-7; the developmentally regulated miR-308 has seed regions completely complementary to the target regions in the 3'UTRs of Acheron (Figure 4). Another developmentally regulated miRNA, miR-2767, has seed regions completely complementary to the target regions in the 3' UTR of Trip-1/SUG1, and miR-92b has seed regions completely complementary to the target regions in the 3'UTR of SCLP (Figure 4). Preliminary data from the Schwartz lab supports the hypothesis that these miRNAs may be key regulators of atrophy and death in the ISMs.

The expression levels of miR-2765 and UCH-7, miR-2767 and Trip-1/SUG1, and miR-92b and SCLP are inversely related (Figure 3). While miR-2767 levels sharply decrease between days 13 to 18 of pupal-adult development, mRNA levels of Trip-1/SUG1 (Figure 3a) increase between days 13 to 18 with the highest level on day 18 shown by the peak in the curve. The same is seen in comparing the levels of miR-2765 with mRNA levels of UCH-7 (Figure 3b), and for comparing the levels of miR-92b and SCLP (Figure 3d). When comparing the mRNA level of Acheron with miR-308 levels (Figure 3c), no inverse relationship is observed. These data are consistent with the hypothesis that miRNAs may play a role in posttranscriptional regulation in the ISMs.

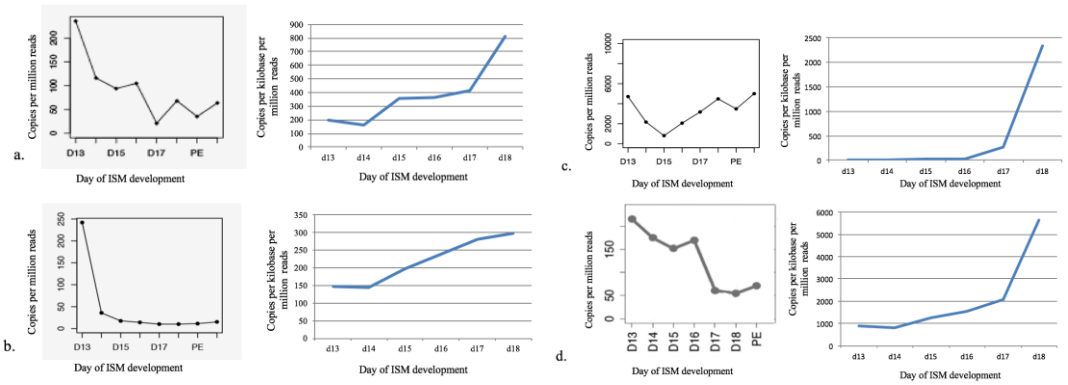

Figure 3. Comparing mRNA and miR levels during ISM development and death. The graphs on the left show the miR levels depicted as reads per million (rpm) vs the day of ISM development (day 13-day 18). The graphs on the right showing the mRNA levels depict reads per kilobase per million reads (RPKM) vs the day of ISM developmental (day 13-day 18 plus 1-hr post-eclosion (PE). The graphs on the left depict: (a) miR-2767 levels, (b) miR-2765 levels, (c) miR-308 levels, and (d) miR-92b levels during development. The graphs on the right depict mRNA levels of the four proteins of interest: (a) Trip-1/SUG1; (b) UCH-7; (c) Acheron; (d) SCLP.

Analysis of Plasmid Constructs and miR targets

Using a bioinformatics approach, putative mRNA targets for the test miRs were identified (Figure 4) and their 3' untranslated region (UTR) were cloned into the pFila plasmid. The putative 22bp mRNA targets were also synthesized and cloned into the pFila plasmid. This plasmid was constructed in such a way that the *Manduca* 3'UTR was cloned downstream of the luciferase gene from the sea pen *Renilla* seen in the pFila map (Figure 5). The plasmid map was generated via SnapGene Viewer (from GSL Biotech; available at snapgene.com).

miR-92b

3′ CGUCCGGCCCUAACCACGUUAA 5′

5′ GUAAGGUCCCUAUAGUGCAAUU 3′

SCLP mRNA

miR-2765

3′ CGGUUGCCACCACCUCAAUGGU 5′

5′ UUCAAUGAUUGUCGAAUUACCA 3′

UCH-7 mRNA

miR 2767

3′ UUUCGGCGUGCUCUAAAUGAAC 5′

5′ ACUAAAUGACUCAUUUUACUUA 3′

Trip-1/SUG1 mRNA

miR-308

3′ GAGCGUCAUAAUAGGACACUAA 5′

5′ CGACUCUGCCUCGACUGUGAUA 3′

Acheron mRNA

Figure 4. MicroRNA putative binding sites. The miRNA targets sites in the 3'UTR of the transcripts were predicted using TargetScan 6.0. The figure shows the miRNA sequences (miR-92b, miR-2767, miR-2765, or miR-308) and their putative mRNA binding sites (SCLP, Trip-1/SUG1, UCH-7, or Acheron). The nucleotides highlighted in yellow indicate mRNA regions complementary to the miRNA seed regions. The blue highlighted regions are miRNA nucleotides that are complementary to the transcripts that are not located in the seed region.

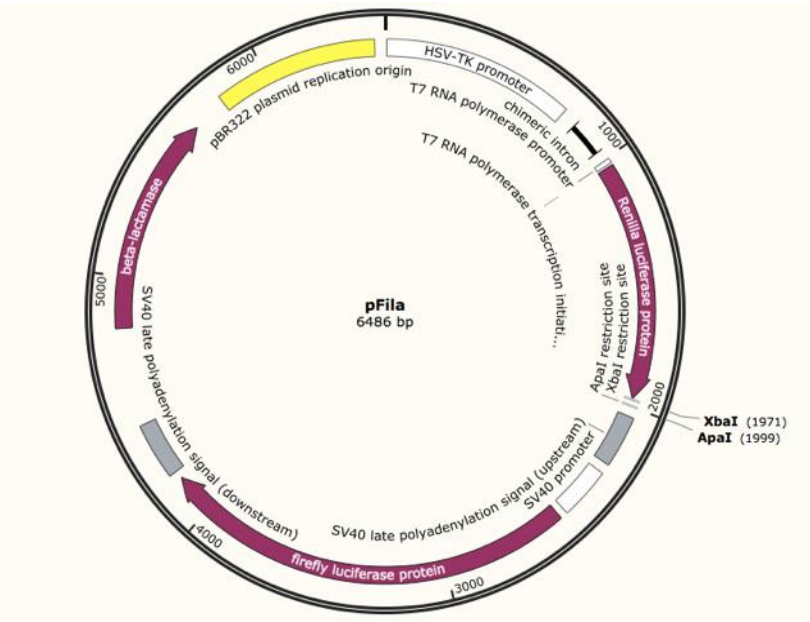

Figure 5. Map of pFila plasmid. The plasmid is constructed in such a way that the *Manduca* 3'UTR of interest was cloned downstream of the luciferase gene from the sea pen *Renilla*. There is also a second constitutively expressed luciferase gene from the firefly. Since both luciferase genes are expressed from the same plasmid within the cell, this is a very robust way to normalize the signal and know what changes are due to the test 3'UTR and what is due to some other experimental variable.

Trip-1/SUG1 protein expression

Using Western blotting we observed that Trip-1/SUG1 expression increases dramatically during day 18 of development when the muscle is committed to die, continuing onto 19 hours post-eclosion (Figure 6). The molecular weight of Trip-1/SUG1 was found to be approximately 45 kDa as expected.

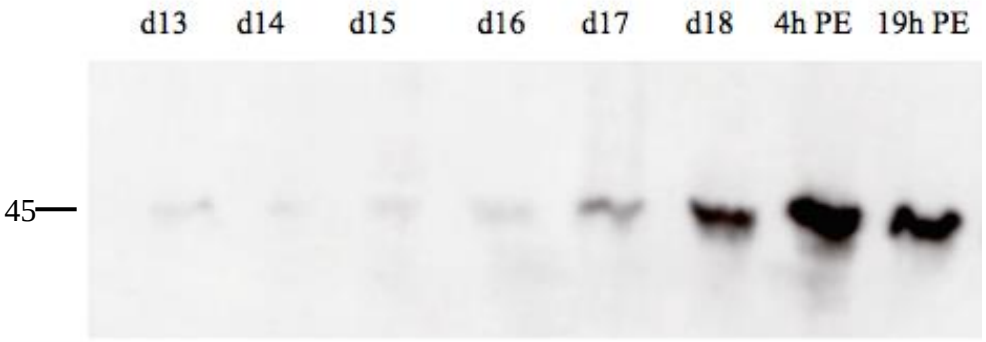

Figure 6. Trip-1/SUG1 protein expression during ISM development. ISM protein (15 ug) was fractionated by SDS PAGE and used to generate a Western blot that was probed with an anti-*Manduca* Trip-1/SUG1. The ECL Western blotting detection system and X-ray film was used to visualize the reaction.

Analysis of luciferase activity

UCH-7

After the COS-1 cells were co-transfected with the engineered constructs and the miRNAs of interest, the cells were assayed to quantify the relative luciferase activity, with and without treatment with miRNAs. Five pFila constructs with different inserts were used when testing each gene of interest. The constructs names for UCH-7 are as follows: 1) UCH7-WT, which has a synthesized 45 nucleotide insert containing the UCH-7 putative miR-2765 binding site; 2) UCH7-3'UTR, which has a ~460 bp insert amplified from 3'UTR; 3) UCH7-siRNA, which has a synthesized 45 nucleotide insert that contains a completely complementary miR-2765 binding site and serves as an siRNA positive control; 4) empty pFila vector, which serves as a negative control; and

5) UCH7-Mutant, which has a synthesized 45 nucleotide insert containing the UCH-7 putative binding site for miR-2765 but with a mutated seed region, which serves as a negative control.

When the cells were co-transfected with UCH7-WT, UCH7-3'UTR, empty pFila vector, and UCH7-Mutant constructs and 1µl of 20nM miR-2765, an increase in luciferase activity was observed, however, it is not statistically significant (Figure 7). When UCH7-siRNA was treated with 1µl of 20nM miR-2765, the relative luciferase activity decreased by 0.69 to 0.31 and was found to be statistically significant (Figure 7).

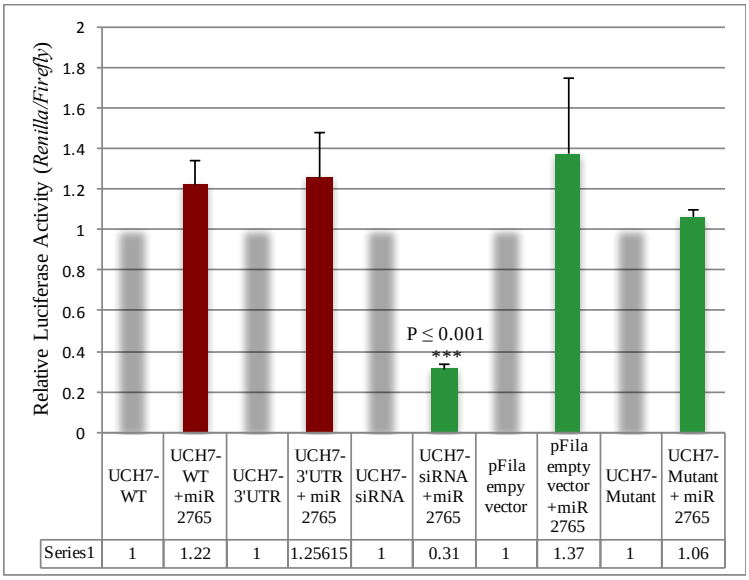

Figure 7. UCH-7 is not post-transcriptionally regulated by miR-2765. The normalized relative luciferase activity (Renilla/firefly) of the UCH-7 constructs when treated with miR-2765 were graphed. The relative luciferase activity was compared after co-transfection of COS-1 cells with the construct (UCH7-WT, UCH7-3'UTR, UCH7-siRNA, empty pFila vector, or UCH7-Mutant) and 1µl of 20nM miR-2765. The student's T-test was used to test statistical significance. The red bars represent the results using the experimental constructs and the green bars represent the results using the control constructs.

Acheron

For Acheron, five constructs were also designed to determine if Acheron is post transcriptionally regulated by miR-308. The constructs names for Acheron are as follows: 1) ACH-WT, which has a synthesized 45 nucleotide insert containing the Acheron putative miR-308 binding site; 2) ACH-3'UTR, which has a ~850bp insert amplified from 3' UTR; 3) ACH-siRNA, which has a synthesized 45 nucleotide insert

completely complementary to miR-308 and serves as a positive siRNA control; 4) empty pFila vector, which serves as a negative control; and 5) ACH-Mutant, which has a synthesized 45 nucleotide insert containing the presumptive Acheron miR-308 binding site but is mutated in the seed region serving as a negative control.

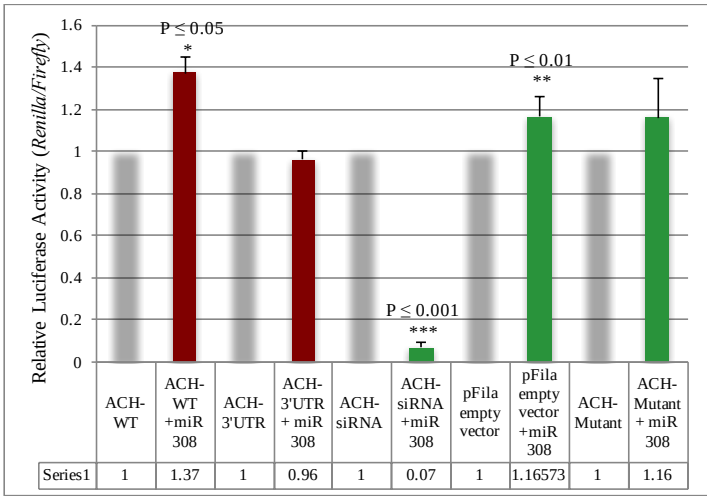

Figure 8. Acheron is not post-transcriptionally regulated by miR-308. The normalized relative luciferase activity (Renilla/ firefly) of the Acheron constructs when treated with miR-308 were graphed. The relative luciferase activity was compared after co-transfection of COS-1 cells with the construct (ACH-WT, ACH-3'UTR, ACH-siRNA, empty pFila vector, or ACH-Mutant) and 1µl of 20nM miR-308. The student's T-test was used to test statistical significance. The red bars represent the results using the experimental constructs and the green bars represent the results using the control constructs.

When the cells were co-transfected with ACH-Mutant and 1µl of 20nM miR-308, an increase in luciferase activity was observed (Figure 8). When the cells were co-transfected with ACH-WT and 1µl of 20nM miR-308, an increase in luciferase activity was observed and was found to be statistically significant (Figure 8). When the cells were co-transfected with the empty pFila vector and 1µl of 20nM miR-308, an increase in luciferase activity was observed and was found to be statistically significant as well (Figure 8). The Acheron/miR-308 siRNA experiment resulted in a 0.93 decrease in luciferase activity to 0.07, which was statistically significant (Figure 8). When ACH-3'UTR was co-transfected with 1µl of 20nM miR-308, the relative luciferase activity decreased 0.04 to 0.96 (Figure 8).

Trip-1/SUG1

For Trip-1/SUG1, five constructs were also designed to determine if Trip-1/SUG1 is post transcriptionally regulated by miR-2767. The constructs names for Trip-1/SUG1 are as follows: 1) SUG1-WT, which has a synthesized 45 nucleotide insert containing the presumptive Trip-1/SUG1 miR-2767 binding site; 2) SUG1-3'UTR, which has a ~600bp insert amplified from the 3' UTR; 3) SUG1-siRNA, which has a synthesized 45 nucleotide insert completely complementary to miR-2767 and serves as an siRNA positive control; 4) empty pFila vector, which serves as a negative control; and 5) SUG1-Mutant, which has a 45 nucleotide insert containing the presumptive miR-2767 Trip-1/SUG1 binding site but with a mutation in the seed region, which serves as a negative control.

When the empty pFila vector was co-transfected with 1µl of 20nM miR-2767, an increase in luciferase activity was observed (Figure 9). When SUG1-WT was co-transfected with 1µl of 20nM miR-2767, the relative luciferase activity decreased by 0.2 to 0.80 (Figure 9). When SUG1-3'UTR, SUG1-siRNA, and SUG1-Mutant were co-transfected with 1µl of 20nM miR-2767, the relative luciferase activity decreased 0.03 to 0.97, 0.82 to 0.18, and 0.08 to 0.92 respectively (Figure 9). The decrease in luciferase activity was found to be statistically significant only when SUG1-WT and Sug1-siRNA were co-transfected with miR-2767 (Figure 9).

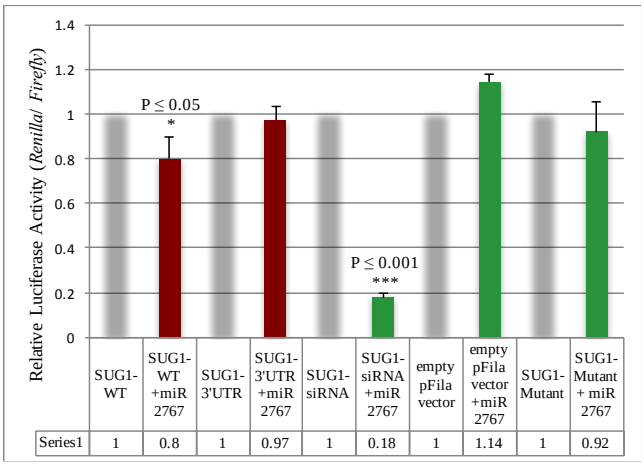

Figure 9. Trip-1/Sug1 may be post-transcriptionally regulated by miR-2767. The normalized relative luciferase activity (Renilla/ firefly) of the Trip-1/SUG1 constructs when treated with miR 2767 were graphed. The relative luciferase activity was compared after co-transfection of COS-1 cells with the construct (SUG1-WT, SUG1-3'UTR, SUG1-siRNA, empty pFila vector, or SUG1-Mutant) and 1µl of 20nM miR-2767. The student's T-test was used to test statistical significance. The red bars represent the results using the experimental constructs and the green bars represent the results using the control constructs.

SCLP

For SCLP, five constructs were also designed to determine if SCLP is post-transcriptionally regulated by miR-92b. The constructs names for SCLP are as follows: 1) SCLP-WT, which has a synthesized 45 nucleotide insert containing the SCLP putative binding site for miR-92b; 2) SCLP-3'UTR, which has a ~400bp insert amplified from ISM cDNA; 3) SCLP-siRNA, which has a synthesized 45 nucleotide insert completely complementary to miR-92b and serves as a positive control; 4) empty pFila vector, which serves as a negative control; and 5) SCLP-Mutant, which has a 45 nucleotide insert containing the SCLP putative binding site for miR-92b but is mutated in the seed region serving as a negative control.

When SCLP-WT, empty pFila vector, and SCLP-Mutant were treated with 1µl of 20nM miR-92b, an increase in luciferase activity was observed (Figure 10). When SCLP-3'UTR and SCLP-siRNA were treated with 1µl of 20nM miR-92b, the relative luciferase activity decreased 0.38 to 0.62 and 0.78 to 0.22 respectively and was found to be statistically significant (Figure 10).

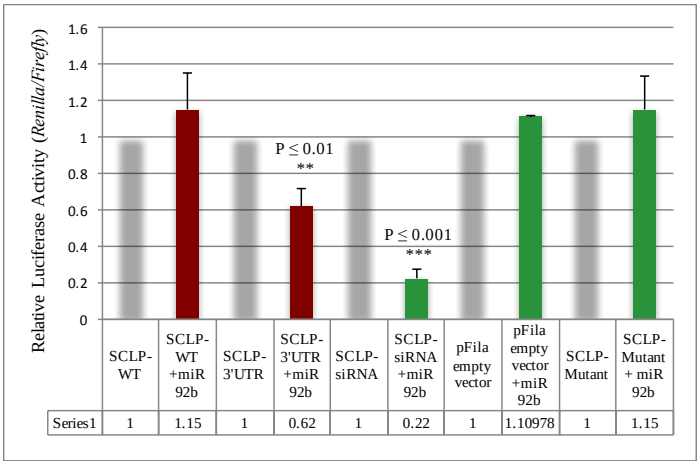

Figure 10. SCLP may be post-transcriptionally regulated by miR-92b. The normalized relative luciferase activity (Renilla/firefly) of the SCLP constructs when treated with miR-92b were graphed. The relative luciferase activity was compared 24 hours after co-transfection of COS-1 cells with the construct (SCLP-WT, SCLP-3'UTR, SCLP-siRNA, empty pFila vector, or SCLP-Mutant) and 1µl of 20nM miR-92b. The student's T-test was used to test statistical significance. The red bars represent the results using the experimental constructs and the green bars represent the results using control constructs.

Quantitative PCR

Quantitative PCR was used to determine if miR-92b affects the stability of SCLP mRNA. *Renilla* expression was normalized to firefly expression and only the constructs SCLP-siRNA and SCLP-3'UTR were used (Figure 11). The COS-1 cells were co-transfected like before with 1µl of 20nM miR-92b and SCLP-siRNA or SCLP-3'UTR. The COS-1 cells were also transfected with only SCLP-siRNA or SCLP-3'UTR and compared to the co-transfection experiment. For SCLP-siRNA with miR-92b, gene expression was observed decreasing 69.30% to 30.90% and was statistically significant (Figure 11). For SCLP-3'UTR with miR-92b, gene expression increased 21.59% but the change was not significant (Figure 11).

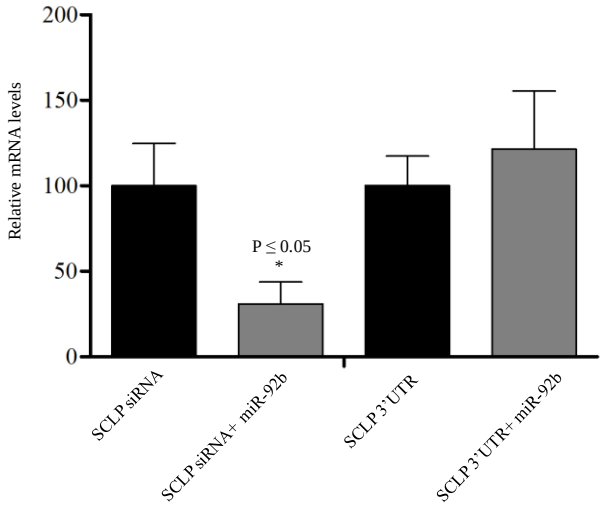

Figure 11. miR-92b has no effect on the transcript stability of SCLP. miR-92b was co-transfected with either SCLP siRNA, a vector with a 3'UTR target site completely complementary to miR-92b, or SCLP 3'UTR, a vector with a 3'UTR target site amplified from ISM cDNA. After 24 hours, the cells were lysed and *Renilla* luciferase expression was measured using SYBR Select Master Mix (Applied Biosystems by Life Technologies, Carlsbad, CA). *Renilla* expression was normalized to firefly expression and relative mRNA levels were compared using the ΔΔCt-method.

Discussion and Implications for Future Research

The molecular mechanisms that regulate programmed cell death during development are poorly understood. It is known that cell death is dependent on *de novo* gene expression of death-associated transcripts (Schwartz et al., 1990a) and these genes have been examined in detail. While many of these changes in gene expression are controlled at the level of transcription, this does not fully account for the changes in gene expression at the protein level. For example, the abundance of the Trip-1/SUG1 mRNA changes two fold between days 17 and 18, rising from 400 RPKM to 800 RPKM (Figure 3a) while the change in protein abundance during that same period increases more than an order of magnitude (Figure 6). One possible mediator of this discrepancy are microRNAs, small interfering RNAs that can block expression post-transcriptionally by blocking translation or facilitating the degradation of target mRNAs (references). Earlier data from the Schwartz lab provided data that is consistent with this hypothesis. They found that there were developmental changes in transcript stability and translatability and that these properties were mediated by sequences within the 3' UTR of ISM genes (Cascone and Schwartz, 2001). However, since they did not evaluate a possible role for miRs Consequently, the focus of my thesis was to directly test this hypothesis. We found that several miRs are developmentally regulated and either declined during ISM development or increased. I chose to focus on the latter since their loss could de-repress transcript expression. As examples, miR-2767 progressively declines during ISM atrophy and death, with the lowest levels on day 17 and day 18 of development (Figure 3a), while miR-92b declines dramatically on day 14 (Figure 3d). miR-2767 targets the Trip-1/SUG1 transcript and mir-92b targets the SCLP transcript.

To functionally test the hypothesis that these developmentally regulated miRs alter the stability or translatability of target mRNAs, I created a series of expression constructs that placed miR target sequences 3' to the *Renilla* luciferase gene in the pFila vector. The vector, with or without the appropriate miR were transfected into COS-1 cells and the subsequent luciferase activity was measured. For each gene studied, I included a vector that contained a sequence that shared 100% complementarity to the miR under investigation, which served as an siRNA positive control. While all of the test miRs display 100% complementary to their putative mRNA targets within the seed region (highlighted in yellow in Figure 4), I did not anticipate that they would alter transcript stability because there is little significant complementarity outside of the seed region (Figure 4).

The functional tests of the pFila vector were successful and I was able to independently detect both *Renilla* and firefly luciferase activities. However, the results I obtained from measuring the effects of miRNA treatment on the target 3' UTRs provided variable results. I expected to observe a decrease in luciferase activity when the cells were treated with the test miRNAs; however, I only observed a statistically significant decrease in luciferase activity for Trip-1/SUG1 and SCLP (Figure 9 and 10).

I found that miR-2765 did not induce a decrease in luciferase activity when the cells were co-transfected with UCH-7 engineered constructs. The only decrease in luciferase expression I observed was when the COS-1 cells were co-transfected with UCH7-siRNA, which has a sequence completely complementary to miR-2765 and acts as an siRNA positive control (Figure 7). As expected, I also observed that miR-2765 had no effect on the luciferase activity when the cells were co-transfected with our

negative controls: the empty pFila vector or the mutant miR target sequence, UCH7-Mutant (Figure 7). Likewise, miR-2765 did not cause a decrease in luciferase activity when the COS-1cells were co-transfected with the experimental constructs UCH7-WT or UCH7-3'UTR, which contains the putative mRNA targets for miR-2765 (Figure 7). Therefore, I conclude that miR-2765 alone does not repress the translatability or stability of the target UCH-7 mRNA because I did not observe a decrease in luciferase activity for our experimental UCH-7 constructs. However, there is a possibility that miR-2765 might act in concert with another miRNA(s) to synergistically induce a decline in the translatability and stability of the target mRNA.

In a separate co-transfection experiment using the construct with the Acheron 3'UTR insert and miR-308 gave a surprising result. I observed a statistically significant increase in luciferase activity when the cells were co-transfected with ACH-WT and miR-308 (Figure 8). However, when I co-transfected the cells with an empty pFila vector, which served as our negative control, I also observed an increase in luciferase activity (Figure 8). Therefore, I believe that miR-308 does not have an effect on the translatability or stability of Acheron mRNA because there was an increase in luciferase activity when the cells were co-transfected in both our experimental and control experiments (Figure 8). However, as mentioned before, there is the possibility that I did not see the expected decrease in luciferase activity because miR-308 only functions combinatorially with other miRs on the Acheron mRNA. For my siRNA control with ACH-siRNA and miR-308, I observed the anticipated decrease in luciferase activity (Figure 8).

For my third set of co-transfection experiments testing Trip-1/SUG1 and miR-2767, I observed a statistically significant decrease in luciferase activity by 0.2 or 20% when I co-transfected my cells with SUG1-WT, the construct with the synthesized putative mRNA binding site for miR-2767, and miR-2767 (Figure 9). I observed the anticipated statistically significant decrease in luciferase activity by 0.82 for our positive siRNA control, SUG1-siRNA, when co-transfected with miR-2767 as expected (Figure 9). I did not see a statistically significant decrease in luciferase activity when SUG1-3'UTR, which has the ~600bp 3' UTR insert, was co-transfected with miR-2767, which may be because miR-2767 has to work in concert with another miR to cause a decrease in the transcript stability and translatability of Trip-1/Sug1 mRNA (Figure 9). Therefore, we conclude that miR-2767 may affect the translatability of Trip-1/SUG1 mRNA. This agrees with our observation of the dramatic increase in Trip-1/SUG1 protein expression seen on the Western blot during through ISM development (Figure 6) and the decrease in miR-2767 levels during atrophy and the commitment to die (Figure 3).

My final gene of interest was SCLP. In contrast to the previous experiments, I observed a decrease in luciferase activity when I co-transfected the cells with SCLP-3'UTR, which has the amplified putative mRNA binding site from ISM cDNA, and miR-92b (Figure 10). However, we did not observe a decrease in luciferase activity when we co-transfected our cells with SCLP-WT, which has the synthesized putative mRNA binding site, which was not expected (Figure 10). One possible reason that may account for the observed the 38% decrease in luciferase activity is the difference in insert size between the two constructs. SCLP-WT has a 45bp insert, while SCLP-3'UTR has a 400bp insert. Because of the shorter insert, SCLP-WT does not provide the full

structural context for proper miR-92b binding, thus we did not see a decrease in luciferase expression for SCLP-WT. (Figure 10). I saw the anticipated decrease in luciferase activity when I co-transfected our cells with our positive siRNA control SCLP-siRNA, and no difference in luciferase activity when I co-transfected our cells for our negative controls empty pFila vector or the SCLP-Mutant, as expected (Figure 10).

I wanted to determine if miR-92b-dependent repression in expression was due to effects on transcript translatability or stability, so I employed qPCR to quantify mRNA levels. I tested SCLP-siRNA as a positive siRNA control and SCLP- 3'UTR as the experimental construct, where I previously observed a 38% decrease in luciferase activity (Figure 10). miR-92b treatment resulted in a 69.30% decrease in transcript abundance for SCLP-siRNA, as expected (Figure 11). However, I did not detect a decrease in gene expression of the SCLP-3'UTR when the cells were co-transfected with SCLP-3'UTR and miR-92b (Figure 11). I interpreted these data as suggesting that while miR-92b blocks SCLP translation, it does not alter transcript stability (Figure 11).

It should be noted that miR-92b is of interest for our study because it has a suggested role in several clinical disorders and a demonstrated regulatory role in apoptosis (Li et al., 2013). miR-92 was found to be highly expressed in high-grade gliomas, an aggressive form of brain tumor (Li et al., 2013). In these tumors, miR-92 was observed to increase glioma cell proliferation and repress apoptosis in glioma (Li et al., 2013). When the cells were treated with a miR-92 inhibitor, the level of apoptosis was increased (Li et al., 2013). To offer more support to the role of miR-92 in apoptosis, the miR-92 family was also found to have a role in regulating the mitochondrial apoptotic machinery via its control on the expression of BIM, which is a pro-apoptotic

BH3-only protein (Pernaute et al., 2014). miR-92 has clinical significance in human muscle disorders as well, as it was found to be repressed in idiopathic dilated cardiomyopathy and ischemic cardiomyopathy, two types of heart failure (Sucharov et al., 2008).

In the future, the lab plans to advance to *in vivo* experiments using the *Manduca* embryo GV1 cell line (Lan et al., 1997). By using GV1 cells, we can determine the functional interaction between ISM miRNAs and mRNAs *in vivo*. We already know that GV1 cells express Acheron, and assume that they express proteasome subunits (Trip-1/Sug1) and likely express UCH-7 as well. It is unknown if they also express SCLP. We also hope to perform combinatorial microRNA experiments using multiple microRNAs to test if multiple microRNAs can have a greater effect in blocking translation or decreasing the transcript stability of our target transcripts.

By determining the functional interaction between miRNAs and mRNAs in the ISMs, we can gain a better understanding about the regulation of skeletal muscle atrophy and death that may provide insights into normal and pathological muscle processes in humans.

Materials and Methods

Western Blot

To determine the Trip-1/SUG1 protein expression in the ISMs during development, tissue was collected from *Manduca* during day 13 to day 18 of development, 4 and 19 hours post-eclosion. Proteins were extracted in Laemlli buffer and 15 ug of each sample were fractionated via gel electrophoresis using a 12% Mini-PROTEAN® TGX™ polyacrylamide gel (Bio-Rad, Hercules, California). Following electrophoresis, the proteins were electrophoretically transferred to Immobilon-P (EMD Millipore) and reacted with a rabbit anti-Trip-1/Sug1 antibody (named 18-56) (Sun et al.,1996) at a 1:2000 dilution followed by detection with goat anti-rabbit antibody (Jackson ImmunoResearch). The Western Lightning™ Plus-ECL, Enhanced Chemiluminescence Substrate (PerkinElmer, Waltham, MA) and X-ray film was used for protein detection.

Engineering constructs

Regions of the target mRNAs containing putative miRNA binding sites were subcloned into the pFila vector. ISM RNA (provided by C. Brown in the Schwartz lab) was used to synthesize the cDNA using reverse transcriptase PCR (RT-PCR). To perform RT-PCR, Superscript III First-Strand Synthesis System (Invitrogen, Carlsbad, CA) was used. Primers were then designed that would amplify the miR-2765 and miR-308 target regions in Acheron, the miR-2765 target region in UCH-7, the miR-2767 and miR-6096 target regions in Trip-1/SUG1, and the miR-92b target region in SCLP (presented below). The miRNA targets sites in the 3'UTR of the transcripts were predicted using TargetScan 6.0 (Lewis et al.,2005). The primers were designed using the

online Integrated DNA Technologies PrimerQuest software (Coralville, IA) and a vector-specific sequence was added onto the 5' end of the primers using In-Fusion Primer Design (Clontech, Mountain View, CA). Primers were then ordered through Integrated DNA technologies (Coralville, IA). The primers used for subcloning the 3'UTR insert of Acheron into the pFila vector were 5'-GAACAATAATTCTAGAGTTGGACAGTGCGAATGTTTAG- 3' and 5'-AAGCGGCCGCTCTAGGGCCCACGAGTGCGACGAAAGTATAG- 3'. The primers used for subcloning the 3'UTR insert of UCH-7 into the pFila vector were 5'-GAACAATAATTCTA GAGCGCGTTGTATAGGGTGATAA- 3' and 5'-AAGCGGCCGCTCTAGGGCCCCCGAACT AAACAGGGCAGAA-3'. The primers used for subcloning the 3'UTR insert of Trip-1/SUG1 into the pFila vector were 5'-GAACAATAATTCTAGGCATAACACAGTCCCTGCATAA-3' and 5'-AAGCGGCCGCTCTAGGCCATGTCATAACCAACACAAAG-3'. The primers used for subcloning the 3'UTR insert of SCLP into the pFila vector were 5'GAACAATAATTC TAGTCTCTATGGACTAAGCCTGTGA 3' and 5' AAGCGGCCGCTCTAGGACACTT AACATAACATCCCAAACC 3'. I refer to these constructs as gene name-3'UTR, hence (ACH-3'UTR, UCH7-3'UTR, SUG1-3'UTR, and SCLP-3'UTR).

The miRNA 3'UTR target regions were amplified via the polymerase chain reaction (PCR) with the conditions as follows: 30 cycles of (98°C for 10 seconds, 55°C for 15 seconds, and 72°C for 1 minute). The resulting PCR products were purified using the NucleoSpin Gel and PCR Clean-Up Kit (Clontech, Mountain View, CA). The pFila plasmid was linearized via restriction digests using the restriction enzymes *Xba*I and

*Apa*I from New England Biolabs (Ipswich, MA). Next, the target 3' UTR regions of Acheron, UCH-7, Trip-1/SUG1, and SCLP were subcloned into the linearized pFila using the In-Fusion® HD Cloning Kit (Clontech, Mountain View, CA), producing three constructs containing the *Manduca* 3' UTR located downstream of the *Renilla* luciferase gene.

Four additional constructs were generated that contained the 22-nucleotide sequence in the 3'UTR that served as the miRNA target for each gene, which was synthesized by Integrated DNA Technologies (Coralville, IA). The synthesized regions of the target mRNAs containing putative miRNA binding sites were subcloned into the pFila vector. Each insert was synthesized with a 5' *Xba*I sticky end and a 3' *Apa*I sticky end. An *Eco*RI restriction site was also inserted into each synthesized insert to confirm that the insert was successfully subcloned into the pFila vector. For the miR- 92b target in the SCLP 3'UTR the synthesized sense strand was 5' CTAGATAGAATTCTA GTGTAAGGTCCCTATAGTGCAATTGGGCC 3', and the synthesized antisense strand was 3'TATCTTAAGATCACATTCCAGGGATATCAC GTTAAC 5'. For the miR-2767 target in the Trip-1/SUG1 3' UTR, the synthesized sense strand was 5' CTAGATAGAATTCTAGTACTAAATGA CTCATTTTACTTAGGGCC 3' and the synthesized antisense strand was 3' TATCTTAAGATCATGATTTACTGAGTAA AATGAATC 5'. For the miR-308 target in the Acheron 3' UTR, the synthesized sense strand was 5' CTAGATAGAATTCT GTCGACTCTGCCTCGACTGTGATAGGGCC 3' and the synthesized antisense strand was 3' TATCTTAAGATCAGCTGAG ACGGAGCTGACACTATC 5'. For the miR-2765 target in the UCH7 3' UTR, the synthesized sense strand was 5' CTAGATAGAATTCTAGTTTCAATG

ATTGTCGAATTACCAGGGCC 3' and the antisense strand was 3' TAT CTTAAGATCAAAGTTACTAACAGCTTAATGGTC 5'. I refer to these constructs as gene name-WT, hence (ACH-WT, UCH-7-WT, SUG1-WT, and SCLP-WT).

As a negative control, four mutant constructs were generated containing the 22-nucleotide sequence in the 3'UTR that served as the miRNA target for each gene, which was synthesized by Integrated DNA Technologies (Coralville, IA). In the mutant synthesized inserts, three nucleotides located in the mRNA region complementary to the miRNA seed region were exchanged from the sense and antisense strand and the middle nucleotide was deleted. The synthesized regions of the target mRNAs containing putative miRNA binding sites were also subcloned into the pFila vector. For the miR-92b target in the SCLP 3'UTR the synthesized sense strand was 5' CTAGATA GAATTCTAGTGTAAGGTCCCTATAGTCTATTGGGCC 3' and the synthesized antisense strand was 3'TATCTTAAGATCACATTCCAGGGAT ATCAGATAA C 5'. For the miR-2767 target in the Sug1/Trp1 3' UTR, the synthesized sense strand was 5' CTAGATAGAATTCTAGTACTAAATGACTCATTTAGTTA GGGCC 3' and the synthesized antisense strand was 3' TATCTTAAGATCATGA TTTACTGAGTAAATCAATC 5'. For the miR-308 target in the Acheron 3' UTR, the synthesized sense strand was 5' CTAGATAGAATTCTAGTCGACT CTGCCTCGACTCCATAGGGCC 3'and the synthesized antisense strand was 3' TATCTTAAGAT CAGCTGAGACGGAGCTGAGGTATC 5'. For the miR-2765 target in the UCH-7 3' UTR, the synthesized sense strand was 5' CTAGATAGAA TTCTAGTTTCAATGATTGTCGAATAGCAGGGCC 3'and the antisense strand was 3' TATCTTAAGATCAAAGTTACTAACAGCTTATCGTC 5'. I refer to these

constructs as gene name-Mutant, hence (ACH-Mutant, UCH7-Mutant, SUG1-Mutant, and SCLP-Mutant).

In addition, constructs were additionally made that contained a target sequence that was 100% complimentary to the 22-nucleotide test miR, which served as an siRNA positive control, and then subcloned into the pFila vector. The inserts were synthesized by Integrated DNA Technologies (Coralville, IA). For the miR- 92b target in the SCLP 3'UTR the synthesized sense strand was 5' CTAGATAGAATTCTAGT GCAGGCCGGGATTGGTGCAATTGGGCC 3' and the synthesized antisense strand was 3' TACTTAAGATCACGTCCGGCCCTAACCACGTT AAC 5'. For the miR-2767 target in the Sug1/Trp1 3' UTR, the synthesized sense strand was 5' CTAGATA GAATTCTAGTAAAGCCGCACGAGATTTACTTGGGGCC 3' and the synthesized antisense strand was 3' TATCTTAAGATCATTTCGGCGTGCTCTAAATGAACC 5'. For the miR-308 target in the Acheron 3' UTR, the synthesized sense strand was 5' CTAGATAGAATTCTAGTCTCGCAGT ATTATCCTGTGATTGGGCC 3'and the synthesized antisense strand was 3' TATCTTAAGATCAGAGCGTCATA ATAGGACACTAAC 5'. For the miR-2765 target in the UCH-7 3' UTR, the synthesized sense strand was 5' CTAGATAGAATTCTAGTGCCAACGGTGGT GGAGTTACCAGGGCC 3'and the antisense strand was 3' TATCTTAAGATCAC GGTTGCCACCACCTCAATGGTC 5'. I refer to these constructs as gene name-siRNA, hence (ACH-siRNA, UCH7-siRNA, SUG1-siRNA, and SCLP-siRNA).

Transformation of Escherichia coli cells

The pFila constructs were transformed into Stellar Competent cells, an *E.coli* HST08 strain obtained from Clontech Laboratories, Inc. (Mountain View, CA). The

bacterial colonies were then mini-prepped to extract the plasmid DNA using the QIAprep Spin Miniprep Kit (QIAGEN,Valencia, CA). Restriction digestions of the three DNA plasmids were then performed to confirm the presence of the anticipated inserts and the digestion products were visualized using agarose gel electrophoresis. The plasmid with the Acheron 3'UTR was digested with *Sac*II, the plasmid with the UCH-7 3'UTR was digested with *Eco*RI, and the plasmid with the Trip-1/SUG1 insert was digested with *Hind*III. The restriction enzymes were all from New England Biolabs (Ipswich, MA). Colony PCR was also used to determine the identity of the inserts. To further verify the identity of the inserts, the purified DNA constructs were sent to Genewiz for sequencing. The bacterial colonies transformed with the correct insert were then maxi-prepped using the EndoFree Plasmid Maxi Kit (QIAGEN, Valencia, CA).

Cell culture, Transfection and Cotransfection of COS-1 cells and Dual Luciferase Assay

COS-1 cells, which are derived from the African green monkey kidney, were grown and maintained in high glucose Dulbecco's Modified Eagle Medium (DMEM) (Gibco, Grand Island, NY) with 10% fetal bovine serum (Atlanta Biologicals, Flowery Branch, GA) and 1X Penicillin/Streptomycin solution (Gibco, Grand Island, NY). In all transfection experiments, 4×10^4 COS-1 cells were seeded the day before transfection. In one set of experiments, the COS-1 cells were transfected with 50 ng of plasmid DNA (either empty pFila vector, SCLP-WT, SCLP-3'UTR, SCLP-siRNA, SCLP-Mutant, SUG1-WT, SUG1-3'UTR, SUG1-siRNA, SUG1-Mutant, ACH-WT, ACH-3'UTR, ACH -siRNA, ACH-Mutant, UCH7-WT, UCH7-3'UTR, UCH7-siRNA, UCH7-Mutant) using 2µL of Lipofectamine 2000 transfection reagent (Thermofisher, Waltham, MA).

In a second set of experiments, the COS-1 cells were co-transfected with 50 ng of DNA (either pFila, SCLP-WT, SCLP-3'UTR, SCLP-siRNA, SCLP-Mutant, SUG1-WT, SUG1-3'UTR, SUG1-siRNA, SUG1-Mutant, ACH-WT, ACH -3'UTR, ACH -siRNA, ACH-Mutant, UCH7-WT, UCH7-3'UTR, UCH7-siRNA, UCH7-Mutant) and 1µl of 20µM miRNA (either miR-92b for SCLP constructs, miR-2767 for Trip1/SUG1 constructs, miR-308 for Acheron constructs, and miR-2765 for UCH-7 constructs) ordered from QIAGEN (Valencia, CA) using 2µL of Lipofectamine 2000 transfection reagent (Thermofisher, Waltham, MA). All transfections were completed in triplicates. The COS-1 cells were collected and lysed 24 hours after transfection with passive lysis buffer (Promega, Madison, WI) To observe the effects of miRNA on luciferase gene expression, the amount of luciferase activity was quantified using the Dual Luciferase Reporter Assay System (Promega, Madison, WI).

Normalizing the Dual luciferase reporter assay

Transfected cells were analyzed by spectrophotometric plate assays (Hofmann et. al., 1999) using the Dual Luciferase Reporter Assay System (Promega, Madison, WI) and the POLARstar Optima microplate reader (BMG Labtech, Cary, NC). To normalize the data for the reporter assays, the fold change in activity was calculated by determining the ratio of *Renilla* luciferase activity (RLU) to firefly luciferase activity of the DNA plasmids following treatment with miRNAs and the ratio of *Renilla* to firefly luciferase activities of the control plasmid without treatment of miRNAs.

Quantitative PCR

Total RNA was isolated from transfected COS-1 cells using the RNeasy Mini Kit (QIAGEN, Valencia, CA). 100 ng of total RNA was used to synthesize the cDNA using RT-PCR. Superscript III First-Strand Synthesis System (Invitrogen, Carlsbad, CA) was used to perform RT-PCR.

Renilla luciferase expression was measured using SYBR Select Master Mix (Applied Biosystems by Life Technologies, Carlsbad, CA). The *Renilla* forward primer used was 5' CATGGGATGAATGGCCTGATA 3' and the *Renilla* reverse primer used was 5' CAACATGGTTTCCACGAAGAAG 3'. *Renilla* expression was normalized to firefly luciferase mRNA expression using ΔΔCt- method. The firefly forward primer used was 5' CATAGCTTACTGGGACGAAGAC 3'. The firefly reverse primer used was 5' CCACCTGATAGCCTTTGTACTT 3'. All experiments were performed with experimental quadruplicates and technical duplicates.

REFERENCES

Bartel, D. (2009). MicroRNAs: Target recognition and regulatory functions. *Cell, 136*, 215-233.

Baumgartner, R. N., Koehler, K., Gallagher, D., Romero, L., Heymsfield, S. B., Ross, R. R., et al. (1998). Epidemiology of sarcopenia among the elderly in new mexico. *American Journal of Epidemiology, 147*(8), 755-763.

Bi, Y., Zheng, X., Shao, C., Pan, W., Jiang, L., & Ouyang, H. (2011). Construction and application of a built-in dual luciferase reporter for microRNA functional analysis. *Electronic Journal of Biotechnology, 14*(2), 1-8.

Cascone, P., & Schwartz, L. M. (2001). Role of the 3′ UTR in regulating the stability and translatability of death-associated mRNAs in moth skeletal muscle. *Development Genes and Evolution, 211,* 397-405.

Filipowicz, W., Bhattacharyya, S., & Sonenberg, N. (2008). Mechanisms of post-transcriptional regulation by microRNAs: Are the answers in sight? *Nature Reviews Genetics, 9,* 102-114.

Hausser, J., & Zavolan, M. (2014). Identification and consequences of miRNA-target interactions [mdash] beyond repression of gene expression. *Nature Reviews Genetics, 15*(9), 599-612.

He, J., Zhu, Q., Wani, G., Sharma, N., & Han, C. (2014). Ubiquitin-specific protease 7 regulates nucleotide excision repair through deubiquitinating XPC protein and preventing XPC protein from undergoing ultraviolet light-induced and VCP/p97 protein-regulated proteolysis. *The Journal of Biological Chemistry, 289*(30).

Hofmann, W., Schubert, D., LaBonte, J., Munson, L., Sodroski, J., Gibson, S., et al. (1999). Species-specific, postentry barriers to primate immunodeficiency virus infection.*Journal of Virology, 73*(12), 10020-10028.

Hughes, V. A., Frontera, W. R., Roubenoff, R., Evans, W. J., & Singh, M. (2002).

Hutvagner, G., & Zamore, P. (2002). A microRNA in a multiple-turnover RNAi enzyme complex. *Science, 297,* 2056-2060.

Lan, Q., Wu, Z. N., & Riddiford, L. M. (1997). Regulation of the ecdysone receptor, USP, E75 and MHR3 mRNAs by 20- hydroxyecdysone in the GV1 cell line of the tobacco hornworm, Manduca sexta. *Insect molecular biology*, *6*(1), 3-10.

Li, Q., Shen, K., Zhao, Y., Ma, C., Liu, J., & Ma, J. (2013). MiR-92b inhibitor promoted glioma cell apoptosis via targeting DKK3 and blocking the Wnt/beta-catenin signaling pathway. *Journal of translational medicine, 11*(1), 1.

Lockshin, R. A., & Williams, C. M. (1965). Programmed cell death—I. Cytology of degeneration in the intersegmental muscles of the Pernyi silkmoth. *Journal of insect physiology, 11*(2), 123-133.

Longitudinal changes in body composition in older men and women: Role of body weight change and physical activity. *The American Journal of Clinical Nutrition, 76*, 473-481.

Janssen, I., Shepard, D. S., Katzmarzyk, P. T., & Roubenoff, R. (2004). The healthcare costs of sarcopenia in the united states.. *Journal of the American Geriatrics Society, 52*(1), 80-85.

Marzetti, E., & Leeuwenburgh, C. (2006). Skeletal muscle apoptosis, sarcopenia and frailty at old age. *Experimental Gerontology, 41*, 1234-1238.

McKenna, N., Lanz, R., & O'Malley, B. (2013). Nuclear receptor coregulators: Cellular and molecular biology. *Endocrine Reviews, 20*(3), 321-344.

Pernaute, B., Spruce, T., Smith, K. M., Sánchez-Nieto, J. M., Manzanares, M., Cobb, B., & Rodríguez, T. A. (2014). MicroRNAs control the apoptotic threshold in primed pluripotent stem cells through regulation of BIM. *Genes & development*, *28*(17), 1873-1878.

Roubenoff, R. (2000). Sarcopenia and its implications for the elderly.. *European Journal of Clinical Nutrition, 54*, S40-S47.

Sayed, D., & Abdellatif, M. (2011). MicroRNAs in development and disease. *Physiological Reviews*, 91(3), 827-887.

Schiaffino, S., Dyar, K., Ciciliot, S., Blaauw, B., & Sandri Marco. (2013). Mechanisms regulating skeletal muscle growth and atrophy. *The FEBS Journal, 280*(17), 4294-4314.

Schwartz, L. M. (2008). Atrophy and programmed cell death of skeletal muscle. *Cell Death and Differentiation, 15*, 1163-1169.

Schwartz, L. M., Jones, M. E., Kosz, L., & Kuah, K. (1993). Selective repression of actin and myosin expression during the programmed death of insect skeletal muscle. . *Developmental Biology, 158*(2), 448-455.

Schwartz, L. M., Kosz, L., & Kay, B. K. (1990). Gene activation is required for developmentally programmed cell death. *Proceedings of the National Academy of Sciences*, *87*(17), 6594-6598.

Schwartz, L. M., Myer, A., Kosz, L., Engelstein, M., & Maier, C. (1990). Activation of polyubiquitin gene expression during developmentally programmed cell death. *Neuron*, *5*(4), 411-419.

Schwartz, L. M., & Ruff, R. L. (2002). Changes in contractile properties of skeletal muscle during developmentally programmed atrophy and death. *American Journal of Physiology-Cell Physiology, 282,* 1270-1277.

Schwartz, L. M., & Truman, J. W. (1983). Hormonal control of rates of metamorphic development in the tobacco hornworm *Manduca sexta* . *Developmental Biology*, *99*(1), 103-114.

Sucharov, C., Bristow, M. R., & Port, J. D. (2008). miRNA expression in the failing human heart: functional correlates. *Journal of molecular and cellular cardiology*, *45*(2), 185-192.

Sun, D., Sathyanarayana, U.G., Johnston, S.A. and Schwartz, L.M. (1996) A member of the phylogenetically conserved CAD family of transcriptional regulators is dramatically upregulated during the programmed cell death of skeletal muscle in the tobacco hawkmoth *Manduca sexta*. *Developmental Biology*, 173:499-509.

SnapGene software (from GSL Biotech; available at snapgene.com)

Tobin, S. L., Cook, P. J., & Burn, T. C. (1990). Transcripts of individual Drosophila actin genes are differentially distributed during embryogenesis.*Developmental genetics*, *11*(1), 15-26.

Valavanis, C., Wang, Z., Sun, D., Vaine, M., & Schwartz, L. (2007). Acheron, a novel member of the lupus antigen family, is induced during the programmed cell death of skeletal muscles in the moth *Manduca sexta*. *Gene, 393*(1-2), 101-109.

Van Rooij, E., & Olson, E. N. (2007). MicroRNAs: powerful new regulators of heart disease and provocative therapeutic targets. *The Journal of clinical investigation*, *117*(9), 2369-2376.

Zhang, S. G., Liu, C. Y., Li, L., Sun, T. W., Luo, Y. G., Yun, W. J., & Zhang, J. Y. (2013). Examination of Artificial MiRNA Mimics with Centered–Site Complementarity for Gene Targeting. *PloS one*, *8*(8), e72062.

Zhang, X., Zheng, Y., Jagadeeswaran, G., Ren, R., Sunkar, R., & Jiang, H. (2012). Identification and developmental profiling of conserved and novel microRNAs in Manduca sexta. *Insect biochemistry and molecular biology*,*42*(6), 381-395.